Bioorganic & Medicinal Chemistry 18 (2010) 8374–8382

Contents lists available at ScienceDirect

Bioorganic & Medicinal Chemistry

journal homepage: www.elsevier.com/locate/bmc

Developing dual functional allosteric modulators of $GABA_A$ receptors

Xiaodong F. Liu [a,*], Hui-Fang Chang [b], Richard Jon Schmiesing [b], Steven S. Wesolowski [b], Katharine S. Knappenberger [a], Jeffrey L. Arriza [a], Marc J. Chapdelaine [b]

[a] Department of Neuroscience Biology, AstraZeneca Pharmaceuticals, Wilmington, DE 19850, USA
[b] Department of Chemistry, AstraZeneca Pharmaceuticals, Wilmington, DE 19850, USA

ARTICLE INFO

Article history:
Received 13 July 2010
Revised 16 September 2010
Accepted 22 September 2010
Available online 29 September 2010

Keywords:
GABAA receptor
Benzodiazepine
Allosteric modulator
Subtype selectivity
Inverse agonist
Cinnoline
Quinoline
Anxiety
Cognition
TEVC

ABSTRACT

Positive modulators at benzodiazepine sites of α2- and α3-containing $GABA_A$ receptors are believed to be anxiolytic. Negative allosteric modulators of α5-containing $GABA_A$ receptors enhance cognition. By oocyte two-electrode voltage clamp and subsequent structure–activity relationship studies, we discovered cinnoline and quinoline derivatives that were both positive modulators at α2-/α3-containing $GABA_A$ receptors and negative modulators at α5-containing $GABA_A$ receptors. In addition, these compounds showed no functional activity at α1-containing $GABA_A$ receptors. Such dual functional modulators of $GABA_A$ receptors might be useful for treating comorbidity of anxiety and cognitive impairments in neurological and psychiatric illnesses.

1. Introduction

$GABA_A$ receptors are pentameric ion channels gated by γ-aminobutyric acid (GABA). There are numerous modulator binding sites on the receptor besides GABA binding sites. Benzodiazepines bind $GABA_A$ receptors allosterically at the interface of α and γ subunits exerting diverse effects in the central nervous system (CNS).[1] Enhancement of $GABA_A$ channel function by positive allosteric modulators (PAMs) at the benzodiazepine site, such as diazepam (Fig. 1), has been a successful therapy to treat anxiety disorders.[2] A few structurally distinct nonbenzodiazepines, such as zolpidem,[3] CGS-9896,[4] TPA023,[5] and α5IA[6] (Fig. 1), can also bind to the benzodiazepine site on $GABA_A$ receptors and modulate various functions of the channel. Although diazepam and other benzodiazepine modulators are often highly efficacious, they also exhibit significant adverse effects such as sedation, amnesia, ataxia, and abuse liability that limit their clinical utility.[7,8] Neurochemical, genetic and pharmacological discoveries indicate that these effects are dissociable according to the α subunit subtype in the pentamer.[9–12] The four major benzodiazepine-sensitive $GABA_A$ receptor subtypes are defined by incorporation of α1, α2, α3, or α5 subunits. The anxiolytic effect of diazepam is mainly mediated by the α2- and α3-containing $GABA_A$ receptors (α2-/α3-$GABA_A$Rs), while the sedation and ataxia effects are primarily mediated by α1-$GABA_A$Rs and the amnesic effect by α1/α5-$GABA_A$Rs (reviewed in Refs. 13 and 14). Compounds made subtype-selective for α2-/α3-$GABA_A$Rs, such as TPA023, have been successfully demonstrated anxiolytic efficacy without sedation in rodents and primates.[5,15] Non-selective negative allosteric modulators (NAMs) of the benzodiazepine site, such as methyl-6,7-dimethoxy-4-ethyl-β-carboline-3-carboxylate (DMCM) (Fig. 1), reportedly have anxiogenic and convulsant liabilities as well as some cognitive enhancement properties.[16] NAMs selective for α5-$GABA_A$Rs (traditionally called α5 inverse agonists) such as α5IA have been shown to be effective in cognitive enhancement in animal models.[6,17] Recently, α5IA has been reported to improve alcohol-induced cognitive impairment without anxiogenesis and convulsion in man.[18] Here we report two new series of nonbenzodiazepine compounds, which are benzodiazepine-site PAMs at α2-/α3-$GABA_A$Rs and NAMs at α5-$GABA_A$Rs with little

Abbreviations: AD, Alzheimer's disease; α_x-$GABA_A$R, α_x-containing $GABA_A$ receptor; CNS, central nervous system; DIEA, *N,N*-diisopropylethylamine; DMCM, methyl-6,7-dimethoxy-4-ethyl-β-carboline-3-carboxylate; DME, dimethoxyethane; DMF, dimethylformamide; GABA, γ-aminobutyric acid; HRMS, high resolution mass spectrometry; NAM, negative allosteric modulator; PAM, positive allosteric modulator; SAR, Structure–activity relationship; TEVC, two-electrode voltage clamp.

* Corresponding author. Tel./fax: +1 302 998 5126.
E-mail addresses: frankliu8@live.com, frank.liu@astrazeneca.com (X.F. Liu).

0968-0896/$ - see front matter © 2010 Elsevier Ltd. All rights reserved.
doi:10.1016/j.bmc.2010.09.058

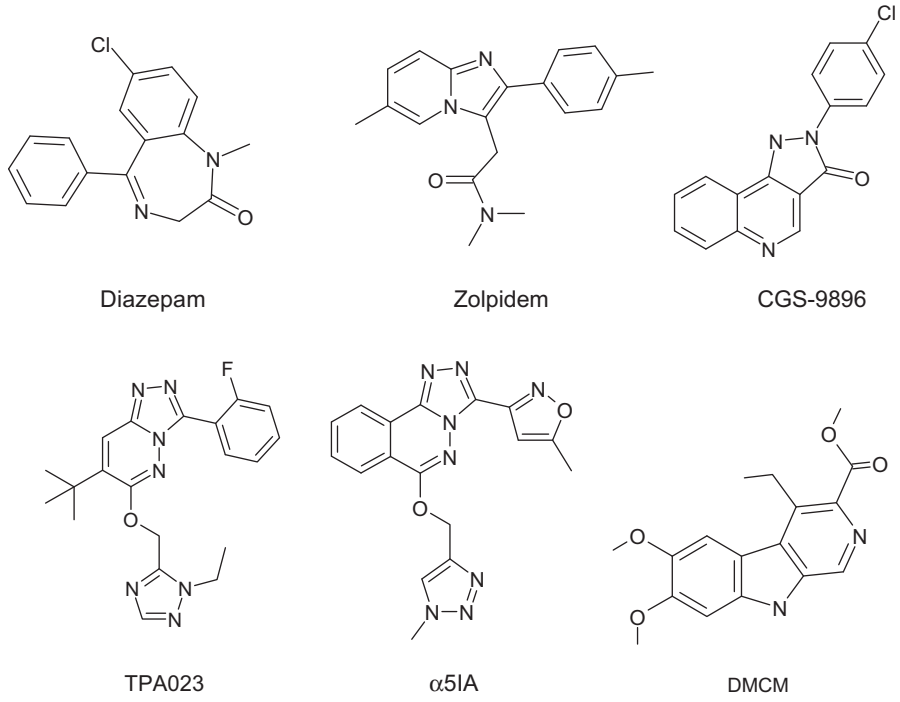

Figure 1. Structures of diazepam and various nonbenzodiazepine modulators at the benzodiazepine site of $GABA_A$ receptors.

functional activity at α1-$GABA_A$Rs. Such molecules are potentially useful in treating cognitive dysfunctions in Alzheimer's disease (AD), with possible added benefit of anxiolysis.

2. Results and discussion

2.1. Chemistry

The chemical synthesis in this report was focused on the formation of biphenyl linkages between heterocyclic groups and the cinnoline or quinoline cores, which was the final step in the synthesis of all compounds **1–13**. Two types of coupling reactions were used for the C–C bond formation. The synthesis of compound **3** was achieved through the Suzuki coupling in 77% yield as outlined in Scheme 1. The Stille coupling was used for the rest of the 12 compounds as described in the Section 4.1.3 and outlined in Scheme 2. Most of the Stille coupling reactions in this study gave yields of 30–60%.

The 8-bromo cinnoline and 5-bromo quinoline precursors used in the coupling reactions were either prepared as described previously[19,20] or as noted in the Section 4.1.2. For the synthesis of compound **2**, the heterocyclic precursor, azetidin-1-yl(5-(trimethylstannyl)pyridin-3-yl)methanone (**2a**), was prepared as outlined in Scheme 3. The synthesis began from 5-bromonicotinic acid, from which 5-bromonicotinoyl chloride was generated by using oxalyl chloride. Azetidine was directly added to the reaction mixture in presence of triethylamine to produce azetidin-1-yl(5-bromopyridin-3-yl)methanone (**2b**) in 71% yield. Finally, displacement of the bromide by a trimethylstannyl group resulted in **2a** in 83% yield.

2.2. Compound screening

In recent years, we have focused on developing PAMs of α2- and α3-$GABA_A$Rs for anxiety treatment with minimum functional activity at α1- and α5-$GABA_A$Rs to reduce side effects such as sedation and amnesia. In this study, a new assay strategy using two-electrode voltage clamp (TEVC) was developed to quickly identify α5-$GABA_A$R NAMs in our compound collection of cinnolines and quinolines that were mainly α2-/α3-$GABA_A$R PAMs and also neutral at α1-$GABA_A$Rs. During the NAM screening, compound **1** (9-amino-2-cyclobutyl-5-(pyrimidin-2-yl)-2,3-dihydro-1*H*-pyrrolo[3,4-*b*]quinolin-1-one) (Scheme 2 and Table 1) and compound **2** (4-amino-8-(5-(azetidine-1-carbonyl)pyridin-3-yl)-*N*-propylcinnoline-3-carboxamide) (Table 1) were identified as NAMs of α5-$GABA_A$Rs. Since they displaced the non-selective benzodiazepine-site modulator [3H]flunitrazepam in the radioligand binding assays, they were most likely benzodiazepine-site modulators.

In case of compound **1**, maximum potentiation for the GABA current at EC_{20} of GABA reached about 40% at both α2- and α3-$GABA_A$Rs with compound's EC_{50} values of 34 and 77 nM,

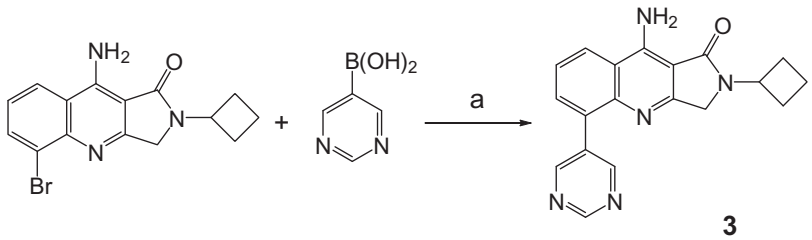

Scheme 1. Reagents and conditions: (a) $Pd(PPh_3)_4$, K_2CO_3, DME/EtOH/H_2O, 90 °C.

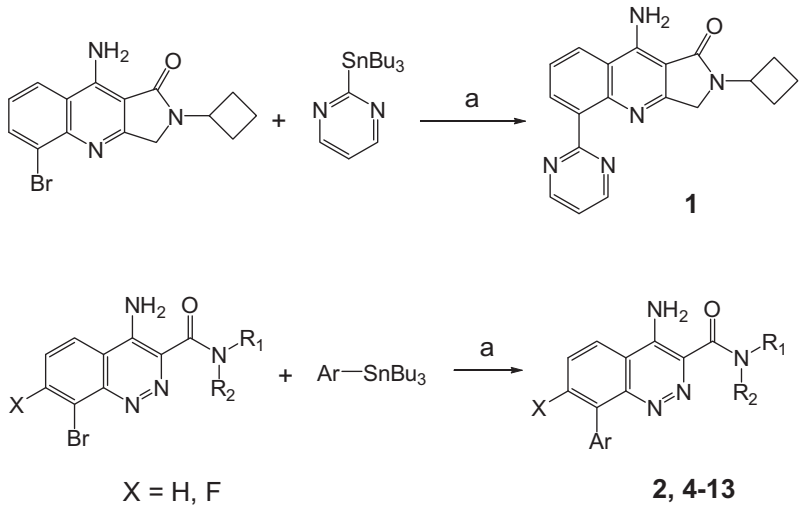

Scheme 2. Reagents and conditions: (a) $Pd(PPh_3)_4$, CuI, DMF, 90–100 °C.

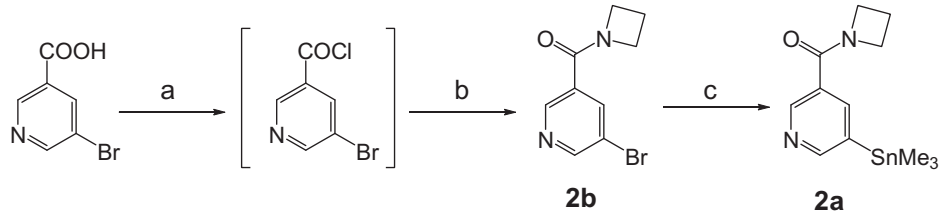

Scheme 3. Reagents and conditions: (a) $(COCl)_2$, CH_2Cl_2, 0 °C; (b) TEA, azetidine, 0 °C to rt; (c) $Pd(PPh_3)_4$, $(SnMe_3)_2$, xylene, 140 °C.

Table 1
Comparing selectivity profiles of diazepam and compounds with significant NAM activities at α5-$GABA_A$Rs[a]

$GABA_A$ subtype	**1**	**2**	**4**	DMCM	Diazepam
	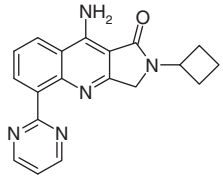	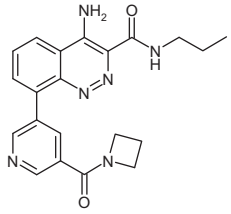	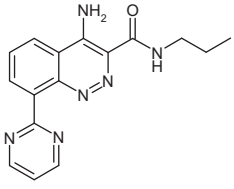	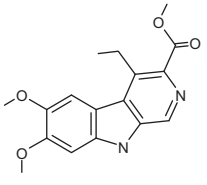	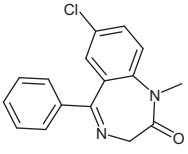
α1β2γ2	1 ± 4; (6)(n/a)[b]	−14 ± 5; (6)(389)	−5 ± 2; (4)(n/a)[b]	−68 ± 2; (4)(9)	192 ± 14; (6)(85)
α2β3γ2	44 ± 5; (4)(34)	−5 ± 3; (6)(54)	22 ± 3; (6)(104)	−61 ± 4; (3)(14)	177 ± 6; (3)(35)
α3β3γ2	40 ± 3; (5)(77)	−11 ± 1; (5)(174)	41 ± 4; (5)(379)	−58 ± 2; (4)(10)	207 ± 24; (5)(131)
α5β3γ2	−46 ± 3; (4)(206)	−45 ± 1; (5)(455)	−52 ± 3; (7)(1130)	−69 ± 2; (4)(3)	153 ± 9; (5)(45)

[a] Data in this table were derived from concentration-response curves (Figs. 2–6). Maximum %modulations and EC_{50} values were obtained by Prism non-linear regression. Data are represented as the best fit value for Top ± Std. error; (number of individual oocytes)(EC_{50} in nM).
[b] Data did not converge. Percent modulation at 1-μM point of the curve was used instead.

respectively (Fig. 2 and Table 1). At α5-$GABA_A$Rs, negative modulation by compound **1** reached −46% with an EC_{50} value of 206 nM. Neither potentiation nor attenuation was observed at α1-$GABA_A$Rs for up to 10 μM of compound **1**. There was no big difference in terms of binding affinity for compound **1** among different subtypes. For example, the K_i values of compound **1** for α2- and α5-$GABA_A$Rs were 8.3 and 14 nM, respectively (Table 2). Compound **2** turned out to be a weak NAM at all subtypes except at the α5-subtype, for which compound **2** showed −45% modulation with an EC_{50} value of 455 nM (Fig. 3 and Table 1).

In parallel experiments, diazepam showed 177% and 153% potentiation for the GABA response at EC_{20} of GABA at α2- and α5-$GABA_A$Rs with EC_{50} values of 35 and 45 nM, respectively (Fig. 4 and Table 1). A non-selective full 'inverse agonist' of $GABA_A$ receptors, DMCM, showed maximum modulation of −61% and −69% with EC_{50} values of 14 and 3 nM at α2- and α5-$GABA_A$Rs, respectively (Fig. 5 and Table 1). The maximum attenuation by compound **1** at α5-$GABA_A$Rs therefore was 67% of the maximum attenuation produced by DMCM. The maximum potentiation by compound **1** at α2-$GABA_A$Rs was 25% of the maximum potentiation exerted by

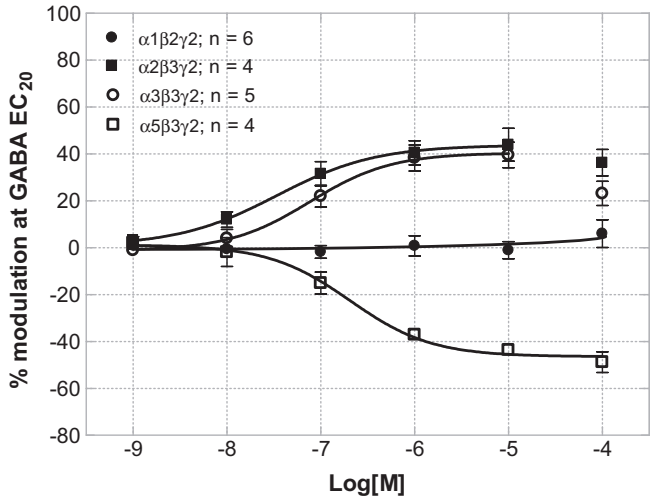

Figure 2. Functional activities of compound **1** measured separately at four different subtypes of human $GABA_A$ receptors expressed in oocytes. Data are represented as Mean ± SEM.

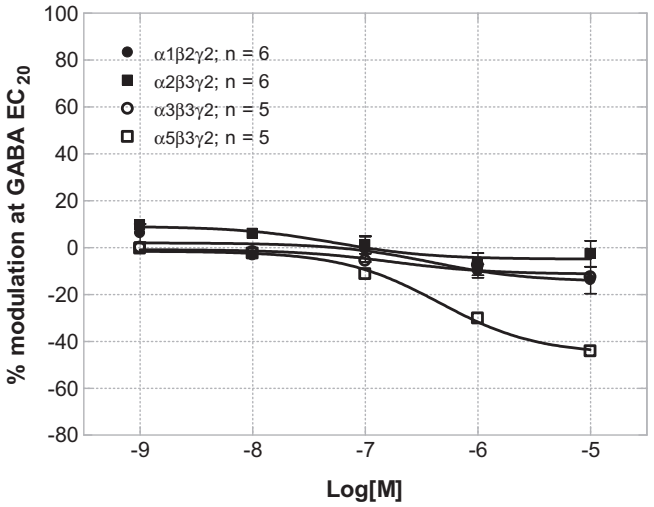

Figure 3. Functional activities of compound **2** measured separately at four different subtypes of human $GABA_A$ receptors expressed in oocytes. Data are represented as Mean ± SEM.

diazepam. Although it is known that 'partial agonists' at the benzodiazepine site on α2-/α3-$GABA_A$Rs are efficacious anxiolytics with less side effects,[21] effectiveness of compounds like **1**, regarding either anxiolytic or cognitive effects, can be further corroborated using relevant animal models and in clinical settings.

2.3. SAR studies for the NAM activity at α5-$GABA_A$Rs

The discovery of compound **1** prompted further investigation. Herein, efforts to improve the overall profile of the modulators by analyzing structure–activity relationships (SAR) are described. Compound **3** (9-amino-2-cyclobutyl-5-(pyrimidin-5-yl)-2,3-dihydro-1*H*-pyrrolo[3,4-*b*]quinolin-1-one) (Scheme 1) differs from compound **1** with respect to the nitrogen positions on the pyrimidine ring. This difference significantly reduced the NAM activity of the compound at α5-$GABA_A$Rs without affecting the binding affinity. One micromolar of compound **3** had only −2% modulation for α5-$GABA_A$Rs with a K_i value of 12 nM while compound **1** showed −32% modulation under the same experimental conditions with a K_i value of 14 nM (Table 2), suggesting that the pyrimidine ring might be the most important side group of compound **1** for its NAM activity at α5-$GABA_A$Rs and the position of the two nitrogen

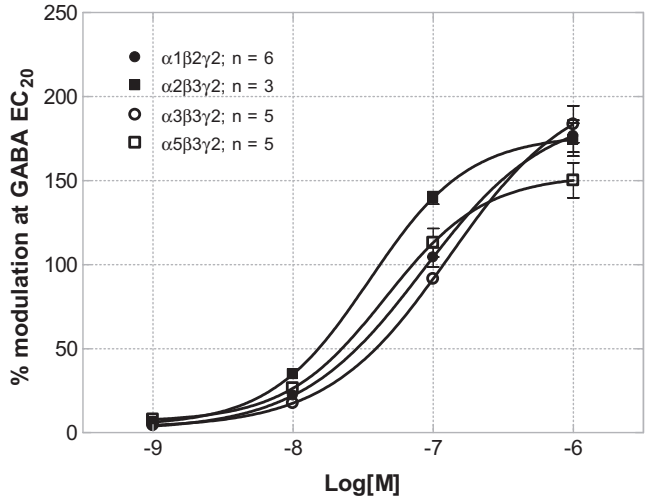

Figure 4. Functional activities of diazepam measured separately at four different subtypes of human $GABA_A$ receptors expressed in oocytes. Data are represented as Mean ± SEM.

Table 2
Impact of the 2-pyrimidyl group on the dual functional activities[a]

Compound	Structure	α5β3γ2		α2β3γ2	
		%modulation	K_i (nM)	%modulation	K_i (nM)
1	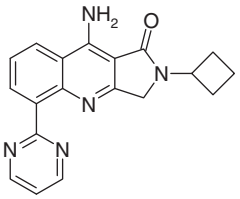	−32 ± 2; (4)	14	38 ± 4; (4)	8.3
3	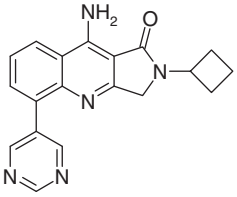	−2 ± 3; (4)	12	18 ± 2; (4)	1.5

[a] Compounds were tested at 1 μM with GABA concentration at EC_{10}. Data are represented as Mean ± SEM; (number of individual oocytes).

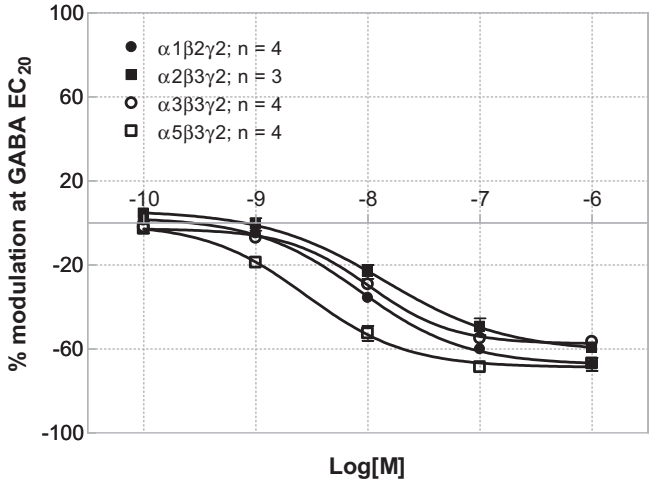

Figure 5. Functional activities of DMCM measured separately at four different subtypes of human $GABA_A$ receptors expressed in oocytes. Data are represented as Mean ± SEM.

atoms proximal to the quinoline core structure could be critical. In addition, since the PAM activity of compound **3** at α2-$GABA_A$Rs was 50% less than compound **1** (Table 2), the 2-pyrimidyl group of compound **1** favored the α2-$GABA_A$R PAM efficacy as well.

These findings were further confirmed when a 2-pyrimidyl group was placed on a cinnoline core structure. By replacing the side group at the 8-position of compound **2** with a 2-pyrimidyl group, we maintained the NAM activity of compound **2** at α5-$GABA_A$Rs, eliminated the NAM activity at α1-$GABA_A$Rs, and enhanced the PAM activities at α2/α3-$GABA_A$Rs. The resulting cinnoline, 4-amino-*N*-propyl-8-(pyrimidin-2-yl)cinnoline-3-carboxamide (**4**)(Table 1), showed 22% potentiation at α2-$GABA_A$Rs with an EC_{50} value of 104 nM, 41% potentiation at α3-$GABA_A$Rs with an EC_{50} value of 379 nM, and −52% modulation at α5-$GABA_A$Rs with an EC_{50} value of 1 μM. Little activity was observed at α1-$GABA_A$Rs for up to 100 μM of compound **4** (Fig. 6).

Attaching a fluoro group at the 7-position of the cinnoline core structure was originally intended for maintaining metabolic stability of the cinnolines. Interestingly, the 7-fluorination reduced the negative modulation and even, in some cases, made compounds positive modulators of α5-$GABA_A$Rs (Table 3), indicating that the negative modulation of α5-$GABA_A$Rs may be affected by the torsional profiles of the pyrimidine ring. Quantum mechanical assessments of conformations of **4** and **9** further illustrate the effect of the fluoro group on the geometries and torsional energy barriers (Section 4.3 and Fig. 7). Compound **4** had lower energy barrier to planarity (3.4 kcal/mol) than compound **9** (9.8 kcal/mol), suggesting that a low energy barrier to planarity might be helpful to the NAM activity. Based on the differences between compounds **1** and **3** and the effects of 7-fluorination on the α5-$GABA_A$R NAM activity, we postulate that the position of the two nitrogen atoms in the pyrimidine ring, approximal to the cinnoline core structure, must play a pivotal role within the receptor in achieving the compound's and/or receptor's active conformation needed for the α5-$GABA_A$R NAM efficacy.

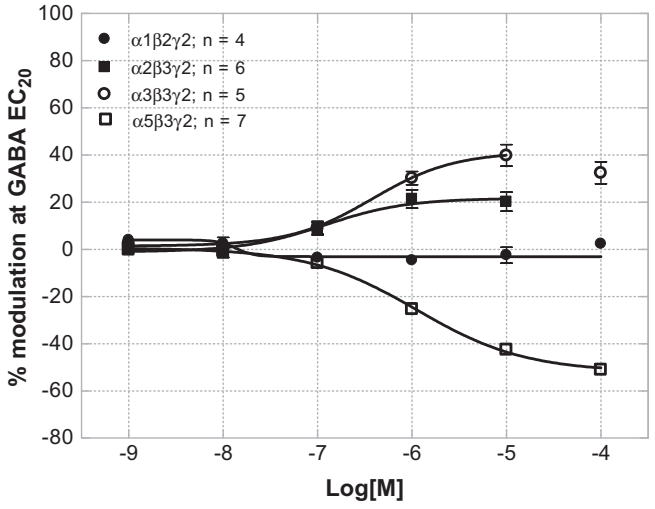

Figure 6. Functional activities of compound **4** measured separately at four different subtypes of human $GABA_A$ receptors expressed in oocytes. Data are represented as Mean ± SEM.

The 7-fluorination also affected the α2/α3-$GABA_A$R PAM activities of compounds **4**–**13** but not as much, percentage wise, as observed for the α5-$GABA_A$R NAM activities (Table 3) and both increased and decreased α2/α3-$GABA_A$R PAM activities were seen upon 7-fluorination. Comparing compounds **4** and **9**, fluorination reduced the α2-$GABA_A$R PAM activity by 47%, indicating that the conformation needed for the α5-$GABA_A$R NAM activity of compound **4** also helped its α2-$GABA_A$R PAM activity. Interestingly, the affinity of compound **9** (K_i = 6 nM) was higher than **4** (K_i = 380 nM) at α2-$GABA_A$Rs. So far, little correlation between binding affinities and functional activities has been observed for these compounds.

The α5-$GABA_A$R NAM and α2-/α3-$GABA_A$R PAM activities of cinnolines **4**–**13** also depended on R1/R2 side groups at the 3-position (Table 3). With 3-methylazetidin-1-yl, *n*-propyl, and azetidin-1-yl groups at R1/R2, compounds **6**, **4**, and **7** showed −35%, −26%, and −22% of α5-$GABA_A$R NAM activities, respectively. In contrast, high α2-$GABA_A$R PAM activities were found in the compounds with R1/R2 of *n*-propyl and cyclopropyl groups. For example, compounds **4** and **5** showed more than 50% potentiation at α2-$GABA_A$Rs. In this study, selection of the side groups at R1/R2 was based on their contribution to the overall selectivity profile. Most of the R1/R2 side groups used in **4**–**13** tend to result in high α2/α3-$GABA_A$R and low α1/α5-$GABA_A$R PAM activities. However, since the side groups at R1/R2 and at the 8-position of cinnolines are both

Table 3
Fluorination reduced the NAM activity at α5-$GABA_A$Rs[a]

NR_1R_2	X	α5β3γ2	α2β3γ2
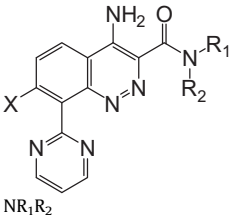	H	**4**: −26 ± 2; (4)	**4**: 58 ± 10; (5)
	F	**9**: −3 ± 4; (4)	**9**: 31 ± 1; (4)
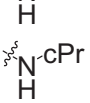	H	**5**: −5 ± 2; (4)	**5**: 54 ± 6; (4)
	F	**10**: 2 ± 5; (3)	**10**: 39 ± 4; (4)
	H	**6**: −35 ± 3; (4)	**6**: 14 ± 2; (4)
	F	**11**: 0 ± 2; (4)	**11**: 18 ± 2; (5)
	H	**7**: −22 ± 1; (4)	**7**: −5 ± 2; (5)
	F	**12**: 10 ± 3; (4)	**12**: 8 ± 1; (4)
	H	**8**: −4 ± 4; (4)	**8**: 6 ± 1; (4)
	F	**13**: 13 ± 4; (3)	**13**: −7 ± 5; (5)

[a] Compounds were tested at 1 μM with GABA concentration at EC_{10}. Data are represented as compound number: Mean of %modulation ± SEM (number of individual oocytes).

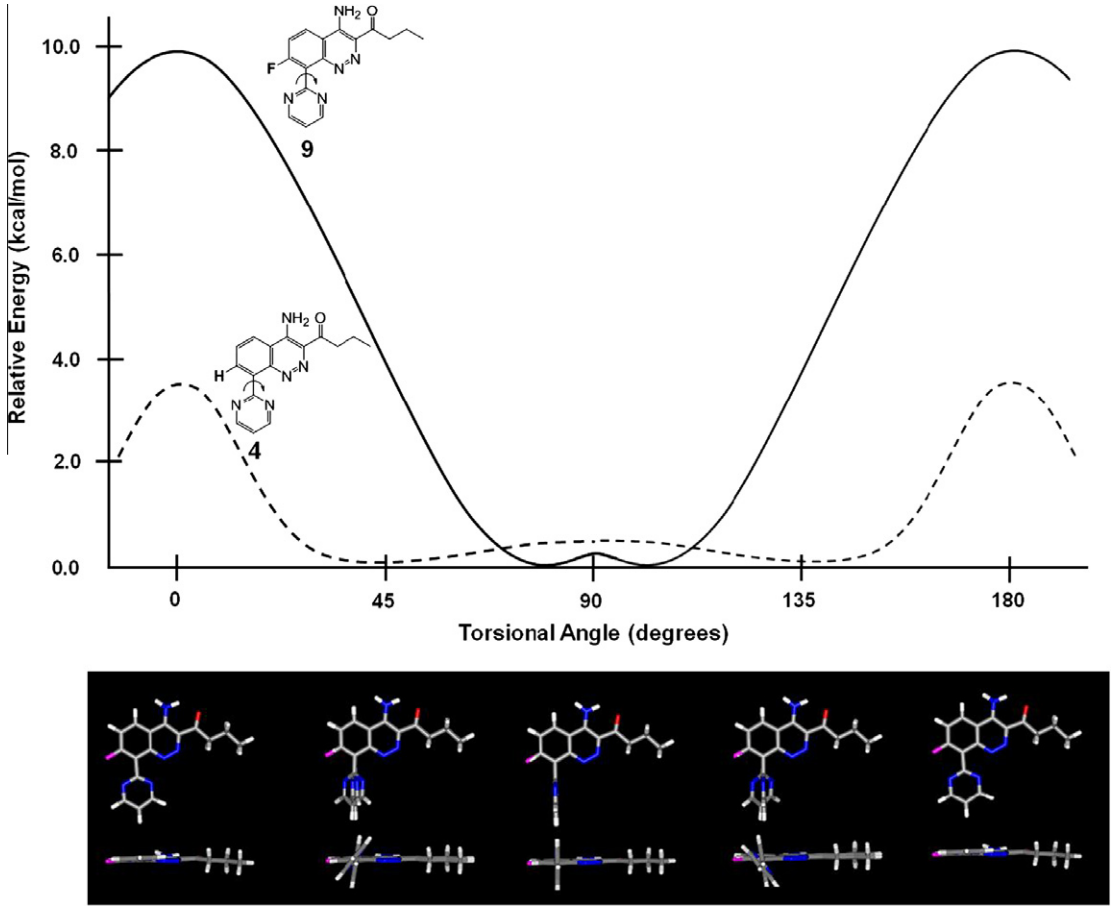

Figure 7. Quantum mechanical simulations of the torsional profiles of compounds **4** (dashed line) and **9** (solid line). Top and side views of the overlays of **4** and **9** are shown for the minima and transition states. The minimum energy structure for **4** has a dihedral angle of ca. 45° whereas the fluorinated compound **9** has a dihedral angle of ca. 75°. In both cases the energy barrier corresponding to orthogonal rings is small (<1 kcal/mol) whereas the barriers to planarity are estimated to be 3.4 and 9.8 kcal/mol for compounds **4** and **9**, respectively. The shapes of these torsional profiles may impact the positive versus negative modulation of α5-$GABA_A$Rs.

important for the functional selectivity, caution must be exercised to make any conclusion for the SAR based solely on R1/R2 variation.

Although dual functional allosteric modulators of $GABA_A$ receptors are technically challenging to develop, the strategy can be an attractive option for treating certain indications in neurological and psychiatric disorders and may offer certain advantages over single functional modulators. Compounds with a subtype selectivity profile like **1** or **4** might be useful when both cognitive enhancement and anxiolysis are needed. For example, clinically relevant levels of anxiety were recorded in 30% of AD patients in addition to their memory loss.[22,23] Besides anxiolytic effects, α2-/α3-$GABA_A$R PAMs have been shown to improve performance in treating cognitive deficits of schizophrenia.[24] It remains to be seen the extent to which improvement of both prefrontal cortical function and hippocampus-dependent memory by a dual functional modulator of $GABA_A$ receptors benefits AD or schizophrenia patients.

Both α5-$GABA_A$Rs and α3-$GABA_A$Rs are believed to impact sensorimotor gating. Yee and co-workers discuss weighing the potential use of α5-$GABA_A$R NAMs to treat hippocampal-related mnemonic dysfunction against the possibility that such compounds may be adversely associated with deficient sensorimotor gating.[25] They also discuss treating sensorimotor-gating deficits with α3-$GABA_A$R PAMs.[26] This and other remaining concerns with α5-$GABA_A$R NAMs such as anxiogenic and pro-convulsion might be addressed by incorporating α2-/α3-$GABA_A$R PAM activities into the same molecule with α5-$GABA_A$R NAMs.

3. Conclusions

In summary, we discovered, in the cinnoline and quinoline series, α5-$GABA_A$R NAMs that also act on α2-/α3-$GABA_A$Rs as PAMs. The subtype selectivity of these dual functional modulators was achieved through differentiation in their functional efficacy rather than their binding affinity. They were benzodiazepine-site 'neutral antagonists' at α1-$GABA_A$Rs and were 'partial agonists' at α2-/α3-$GABA_A$Rs and 'partial inverse agonists' at α5-$GABA_A$Rs in comparison to diazepam and DMCM, respectively. SAR studies revealed that the pyrimidine side group at the 5-position of quinoline and 8-position of cinnoline was important for the dual functional activities, especially for the NAM activity at α5-$GABA_A$Rs. The alignment of the two nitrogen atoms in the 2-pyrimidyl ring with the cinnoline or quinoline core structures may impact the compound's efficacy as α5-$GABA_A$R NAMs.

4. Experimental

4.1. Chemistry

4.1.1. General

All chemicals and reagents were purchased from Sigma-Aldrich, Fisher Scientific Inc., Strem Chemicals, Matrix Scientific, ACE Synthesis, and Frontier Scientific Inc. All reactions were carried out under a nitrogen atmosphere. Silicycle SillaFlash® cartridges were used for flash chromatography. ^{1}H NMRs were obtained on

a Bruker Avance DPX300 NMR or on a Bruker Avance II 500 NMR, and were consistent with the assigned structures. All NMRs were recorded in $CDCl_3$ or DMSO-d_6 unless otherwise specified. High resolution mass spectrometry (HRMS) were determined on an Agilent Technologies 6210 Time-of-Flight LC/MS; its HPLC was conducted using an Agilent SB C-8 analytical column (2.1 × 30 mm, 1.8 μm) and eluting from 5% to 95% methanol (containing 0.1% formic acid) on a 2 min run (1.2 mL/min).

4.1.2. Typical preparation of bromo azetidine precursor

To the corresponding 8-bromo-3-carboxylic acid (1 equiv) in dimethylformamide (DMF) at 0 °C was added in one portion carbonyldiimidazole (1.6 equiv), mixture stirred at 0 °C for 15 min, ice bath removed and stirred at room temperature for 2 h (becomes turbid). To this turbid mixture at 0 °C was added in one portion a preformed solution of the azetidine (1.1 equiv) and *N*,*N*-diisopropylethylamine (DIEA) (1.1 equiv) in DMF. The reaction concentration was 0.3 M. The pale yellow clearing solution was allowed to warm to room temperature, monitoring by LC/MS. Upon completion, the volatiles were removed in vacuo to give a crude product residue which was subjected to a silica gel column eluting with a 0–50% ethyl acetate in methylene chloride gradient to give a solid as the desired product.

4.1.3. General procedure A for the Stille coupling

The corresponding bromide (1 equiv), the corresponding tributylstannyl reagent (2.2 equiv), tetrakis(triphenylphosphine) palladium(0) (0.1 equiv) and copper(I) iodide (0.2 equiv) in DMF were heated at 90–100 °C, monitoring by LC/MS. The reaction concentration was 0.3 M. Upon completion, the reaction mixture was cooled to room temperature, diluted with chloroform (200 mL) and washed with a minimal volume of ammonium hydroxide and water (100 mL × 3). The chloroform layer was dried with magnesium sulfate, and evaporated to constant mass. The crude product was loaded to a silica gel column, and eluted with 0–10% methanol in methylene chloride to give a yellow or tan solid. The solid was further purified by HPLC, and eluted with 5–100% acetonitrile in water to give a white or yellow solid as the desired product.

4.1.4. 9-Amino-2-cyclobutyl-5-(pyrimidin-2-yl)-2,3-dihydro-1*H*-pyrrolo[3,4-*b*]quinolin-1-one (1)

Compound **1** was synthesized in 9% yield from 9-amino-5-bromo-2-cyclobutyl-2,3-dihydro-1*H*-pyrrolo[3,4-*b*]quinolin-1-one[19] and 2-(tributylstannyl)pyrimidine according to the general procedure A. ^{1}H NMR (500 MHz, chloroform-*d*) δ ppm 1.65–1.83 (m, 2H), 2.17–2.33 (m, 4H), 4.46 (s, 2H), 4.90 (quin, *J* = 8.7 Hz, 1H), 6.41 (br s, 2H), 7.33 (t, *J* = 5.0 Hz, 1H), 7.56 (dd, *J* = 8.2, 7.3 Hz, 1H), 7.96 (t, *J* = 7.2 Hz, 2H), 8.93 (d, *J* = 4.9 Hz, 2H); HRMS (ESI, Pos) *m*/*z* 332.1515 (MH+); HPLC 0.74 min.

4.1.5. 4-Amino-8-(5-(azetidine-1-carbonyl)pyridin-3-yl)-*N*-propylcinnoline-3-carboxamide (2)

Compound **2** was synthesized in 44% yield from 4-amino-8-bromo-*N*-propylcinnoline-3-carboxamide[20] and azetidin-1-yl(5-(tributylstannyl)pyridin-3-yl)methanone (**2a**) according to the general procedure A. ^{1}H NMR (300 MHz, chloroform-*d*) δ ppm 1.02 (t, *J* = 7.4 Hz, 3H), 1.63–1.75 (m, 2H), 2.40 (quin, *J* = 7.8 Hz, 2H), 3.48 (q, *J* = 6.7 Hz, 2H), 4.28 (br s, 2H), 4.46 (br s, 2H), 7.69–7.89 (m, 2H), 7.95 (d, *J* = 8.1 Hz, 1H), 8.40 (s, 1H), 8.50 (br s, 1H), 8.89 (br s, 1H), 9.00 (br s, 1H); HRMS (ESI, Pos) *m*/*z* 391.19 (MH+); HPLC 0.88 min.

4.1.5.1. Azetidin-1-yl(5-(trimethylstannyl)pyridin-3-yl)methanone (2a). Compound **2b** (670 mg, 2.50 mmol), hexamethyldistannane (1.58 g, 4.50 mmol) and tetrakis(triphenylphosphine) palladium(0) (140 mg, 0.25 mmol) in xylene (40 mL) were refluxed at 140 °C overnight. Upon completion, the reaction mixture was cooled to room temperature, washed with water (100 mL × 3), dried through magnesium sulfate, and evaporated to dryness. The crude product was loaded onto a silica gel column, and eluted with 0–100% ethyl acetate in hexane to give **2a** in 83% overall yield (846 mg). ^{1}H NMR (300 MHz, DMSO-d_6) δ ppm 0.33 (s, 9H), 2.26 (quin, *J* = 7.7 Hz, 2H), 4.06 (t, *J* = 7.5 Hz, 2H), 4.31 (t, *J* = 7.6 Hz, 2H), 7.94–8.12 (m, 1H), 8.68 (dd, *J* = 3.2, 1.9 Hz, 2H).

4.1.5.2. Azetidin-1-yl(5-bromopyridin-3-yl)methanone (2b). 5-Bromonicotinic acid (1.0 g, 4.95 mmol) was suspended in methylene chloride (15 mL) at 0 °C. Oxalyl chloride (817 mg, 6.44 mmol) was added and stirred at 0 °C for 30 min. Triethylamine (1.252 g, 12.38 mmol) was added, and then azetidine (565 mg, 9.9 mmol) was added at 0 °C. The reaction was warmed to room temperature for 2 h, and then quenched with water. The reaction mixture was diluted with methylene chloride (200 mL), washed with 10% potassium carbonate, dried with magnesium sulfate, and evaporated to dryness. The crude product was loaded to a silica gel column, and eluted with 0–10% methanol in methylene chloride to give **2b** in 71% overall yield (846 mg). ^{1}H NMR (300 MHz, DMSO-d_6) δ ppm 2.27 (dt, *J* = 15.6, 7.8 Hz, 2H), 4.07 (t, *J* = 7.8 Hz, 2H), 4.34 (t, *J* = 7.6 Hz, 2H), 8.20 (t, *J* = 2.0 Hz, 1H), 8.76 (d, *J* = 1.8 Hz, 1H), 8.83 (d, *J* = 2.3 Hz, 1H).

4.1.6. 9-Amino-2-cyclobutyl-5-(pyrimidin-5-yl)-2,3-dihydro-1*H*-pyrrolo[3,4-*b*]quinolin-1-one (3)

9-Amino-5-bromo-2-cyclobutyl-2,3-dihydro-1*H*-pyrrolo[3,4-*b*]quinolin-1-one[19] (250 mg, 0.75 mmol), pyrimidine-5-boronic acid (186 mg, 1.51 mmol), potassium carbonate (624 mg, 4.52 mmol) and tetrakis(triphenylphosphine)palladium(0) (43.5 mg, 0.04 mmol) were added to dimethoxyethane (DME) (3 mL)/water (1.286 mL)/ethanol (0.857 mL) to give a yellow suspension. The reaction mixture was heated to 90 °C as a yellow solution for 2 h. The reaction mixture was cooled to room temperature, evaporated, all of the solvent removed and the residue dissolved in methylene chloride (200 mL). The methylene chloride solution was washed with saturated sodium bicarbonate (20 mL × 2) and brine (20 mL), dried with magnesium sulfate, filtered and concentrated. The crude product was loaded to a silica gel column and eluted with 30–100% ethyl acetate in hexane to give a brown solid (210 mg). The brown solid was further crystallized from diethyl ether/methylene chloride (4 mL/1 mL) at 0 °C overnight to give a white solid as the desired product, which was dried at 90 °C under high vacuum overnight to give **3** (193 mg; 77% yield). ^{1}H NMR (300 MHz, chloroform-*d*) δ ppm 1.70–1.92 (m, 2H), 2.17–2.39 (m, 4H), 4.44 (s, 2H), 4.91 (quin, *J* = 8.5 Hz, 1H), 6.45 (br s, 2H), 7.58 (dd, *J* = 8.3, 7.3 Hz, 1H), 7.76 (dd, *J* = 7.2, 1.3 Hz, 1H), 7.93 (dd, *J* = 8.3, 1.4 Hz, 1H), 9.09 (s, 2H), 9.23 (s, 1H); HRMS (ESI, Pos) *m*/*z* 332.1515 (MH+); HPLC 0.81 min.

4.1.7. 4-Amino-*N*-propyl-8-(pyrimidin-2-yl)cinnoline-3-carboxamide (4)

Compound **4** was synthesized in 49% yield from 4-amino-8-bromo-*N*-propylcinnoline-3-carboxamide[20] and 2-(tributylstannyl)pyrimidine according to the general procedure A. ^{1}H NMR (300 MHz, chloroform-*d*) δ ppm 8.96 (d, *J* = 4.8 Hz, 2H), 8.55 (br s, 1H), 8.09 (dd, *J* = 7.2, 1.1 Hz, 1H), 7.98 (dd, *J* = 8.4, 1.3 Hz, 1H), 7.74 (dd, *J* = 8.4, 7.2 Hz, 1H), 7.35 (t, *J* = 5.0 Hz, 1H), 3.45 (q, *J* = 6.9 Hz, 2H), 1.58–1.72 (m, 2H), 0.99 (t, *J* = 7.4 Hz, 3H); HRMS (ESI, Pos) *m*/*z* 309.15 (MH+); HPLC 0.70 min.

4.1.8. 4-Amino-*N*-cyclopropyl-8-(pyrimidin-2-yl)cinnoline-3-carboxamide (5)

Compound **5** was synthesized in 58% yield from 4-amino-8-bromo-*N*-cyclopropylcinnoline-3-carboxamide[20] and 2-(tributylstannyl) pyrimidine according to the general procedure A. ^{1}H NMR (300 MHz, chloroform-*d*) δ ppm 8.96 (d, *J* = 4.8 Hz, 2H), 8.55 (br s,

1H), 8.10 (dd, J = 7.1, 1.2 Hz, 1H), 7.98 (dd, J = 8.5, 1.2 Hz, 1H), 7.78 (dd, J = 8.4, 7.2 Hz, 1H), 7.36 (t, J = 5.0 Hz, 1H), 2.91–3.03 (m, J = 7.3, 7.3, 3.8, 3.8, 3.7 Hz, 1H), 0.83–0.92 (m, 2H), 0.58–0.67 (m, 2H); HRMS (ESI, Pos) m/z 306.12 (MH+); HPLC 0.63 min.

4.1.9. (4-Amino-8-(pyrimidin-2-yl)cinnolin-3-yl)(3-methylazetidin-1-yl)methanone (6)

Compound **6** was synthesized in 31% yield from (4-amino-8-bromocinnolin-3-yl)(3-methylazetidin-1-yl)methanone and 2-(tributylstannyl)pyrimidine according to the general procedure A. ^{1}H NMR (300 MHz, chloroform-d) δ ppm 1.29 (d, J = 6.9 Hz, 3H), 2.70–2.84 (m, J = 13.7, 6.8, 1.3, 1.3 Hz, 1H), 3.81 (dd, J = 10.2, 5.4 Hz, 1H), 4.38 (td, J = 9.3, 0.8 Hz, 1H), 4.44–4.51 (m, 1H), 4.91–5.02 (m, 1H), 7.35 (t, J = 4.9 Hz, 1H), 7.74 (dd, J = 8.4, 7.2 Hz, 1H), 8.00–8.07 (m, 1H), 8.09–8.15 (m, 1H), 8.95 (d, J = 4.9 Hz, 2H); HRMS (ESI, Pos) m/z 321.15 (MH+); HPLC 0.74 min.

4.1.10. (4-Amino-8-(pyrimidin-2-yl)cinnolin-3-yl)(azetidin-1-yl)methanone (7)

Compound **7** was synthesized in 62% yield from (4-amino-8-bromocinnolin-3-yl)(azetidin-1-yl)methanone and 2-(tributylstannyl)pyrimidine according to the general procedure A. ^{1}H NMR (300 MHz, chloroform-d) δ ppm 2.29–2.42 (m, 2H), 4.25–4.33 (m, 2H), 4.84–4.93 (m, 2H), 7.34 (t, J = 4.9 Hz, 1H), 7.73 (dd, J = 8.4, 7.2 Hz, 1H), 7.98 (d, J = 8.1 Hz, 1H), 8.08 (d, J = 7.1 Hz, 1H), 8.95 (d, J = 4.9 Hz, 2H); HRMS (ESI, Pos) m/z 306.12 (MH+); HPLC 0.64 min.

4.1.11. (4-Amino-8-(pyrimidin-2-yl)cinnolin-3-yl)(3,3-difluoroazetidin-1-yl)methanone (8)

Compound **8** was synthesized in 42% yield from (4-amino-8-bromocinnolin-3-yl)(3,3-difluoroazetidin-1-yl)methanone and 2-(tributylstannyl)pyrimidine according to the general procedure A. ^{1}H NMR (300 MHz, DMSO-d_6) δ ppm 4.46–4.61 (m, 2H), 4.91–5.09 (m, 2H), 7.59 (t, J = 4.9 Hz, 1H), 7.85 (t, J = 7.7 Hz, 1H), 7.97–8.09 (m, 1H), 8.57 (d, J = 8.2 Hz, 1H), 8.74 (br s, 2H), 8.98 (d, J = 4.8 Hz, 2H); HRMS (ESI, Pos) m/z 342.10 (MH+); HPLC 0.68 min.

4.1.12. 4-Amino-7-fluoro-*N*-propyl-8-(pyrimidin-2-yl)cinnoline-3-carboxamide (9)

Compound **9** was synthesized in 54% yield from 4-amino-8-bromo-7-fluoro-*N*-propylcinnoline-3-carboxamide[20] and 2-(tributylstannyl)pyrimidine according to the general procedure A. ^{1}H NMR (300 MHz, chloroform-d) δ ppm 8.98 (d, J = 5.1 Hz, 2H), 8.44 (t, J = 4.7 Hz, 1H), 7.98 (dd, J = 9.3, 5.3 Hz, 1H), 7.52 (d, J = 9.1 Hz, 1H), 7.41 (t, J = 5.0 Hz, 1H), 3.36–3.49 (m, 2H), 1.58–1.68 (m, 2H), 0.98 (t, J = 7.4 Hz, 3H); HRMS (ESI, Pos) m/z 326.13 (MH+); HPLC 0.66 min.

4.1.13. 4-Amino-*N*-cyclopropyl-7-fluoro-8-(pyrimidin-2-yl)cinnoline-3-carboxamide (10)

Compound **10** was synthesized in 47% yield from 4-amino-8-bromo-*N*-cyclopropyl-7-fluorocinnoline-3-carboxamide[20] and 2-(tributylstannyl)pyrimidine according to the general procedure A. ^{1}H NMR (300 MHz, chloroform-d) δ ppm 8.97 (d, J = 5.1 Hz, 2H), 8.42 (d, J = 3.0 Hz, 1H), 7.98 (dd, J = 9.4, 5.2 Hz, 1H), 7.35–7.52 (m, 2H), 2.81–3.02 (m, J = 7.3, 7.3, 3.9, 3.8, 3.7 Hz, 1H), 0.81–0.89 (m, 2H), 0.56–0.66 (m, 2H); HRMS (ESI, Pos) m/z 324.11 (MH+); HPLC 0.57 min.

4.1.14. (4-Amino-7-fluoro-8-(pyrimidin-2-yl)cinnolin-3-yl)(3-methylazetidin-1-yl)methanone (11)

Compound **11** was synthesized in 28% yield from (4-amino-8-bromo-7-fluorocinnolin-3-yl)(3-methylazetidin-1-yl)methanone and 2-(tributylstannyl)pyrimidine according to the general procedure A. ^{1}H NMR (300 MHz, chloroform-d) δ ppm 8.96 (d, J = 4.9 Hz, 2H), 7.96 (dd, J = 9.2, 5.3 Hz, 1H), 7.51 (t, J = 8.9 Hz, 1H), 7.39 (t, J = 4.9 Hz, 1H), 4.89 (dd, J = 10.0, 8.5 Hz, 1H), 4.28–4.48 (m, 2H), 3.79 (dd, J = 9.9, 5.6 Hz, 1H), 2.62–2.85 (m, 1H), 1.27 (d, J = 7.0 Hz, 3H); HRMS (ESI, Pos) m/z 338.13 (MH+); HPLC 0.78 min.

4.1.15. (4-Amino-7-fluoro-8-(pyrimidin-2-yl)cinnolin-3-yl)(azetidin-1-yl)methanone (12)

Compound **12** was synthesized in 20% yield from (4-amino-8-bromo-7-fluorocinnolin-3-yl)(azetidin-1-yl)methanone and 2-(tributylstannyl)pyrimidine according to the general procedure A. ^{1}H NMR (300 MHz, chloroform-d) δ ppm 8.96 (d, J = 4.9 Hz, 2H), 7.97 (dd, J = 9.3, 5.2 Hz, 1H), 7.51 (t, J = 8.9 Hz, 1H), 7.39 (t, J = 5.0 Hz, 1H), 4.82 (t, J = 7.7 Hz, 2H), 4.27 (t, J = 7.7 Hz, 2H), 2.34 (quin, J = 7.8 Hz, 2H); HRMS (ESI, Pos) m/z 324.11 (MH+); HPLC 0.55 min.

4.1.16. (4-Amino-7-fluoro-8-(pyrimidin-2-yl)cinnolin-3-yl)(3,3-difluoroazetidin-1-yl)methanone (13)

Compound **13** was synthesized in 37% yield from (4-amino-8-bromo-7-fluorocinnolin-3-yl)(3,3-difluoroazetidin-1-yl)methanone and 2-(tributylstannyl)pyrimidine according to the general procedure A. ^{1}H NMR (300 MHz, DMSO-d_6) δ ppm 4.52 (t, J = 12.3 Hz, 2H), 4.96 (t, J = 12.3 Hz, 2H), 7.63 (t, J = 5.0 Hz, 1H), 7.81 (t, J = 9.1 Hz, 1H), 8.65 (dd, J = 9.4, 5.6 Hz, 1H), 9.00 (d, J = 5.0 Hz, 2H); HRMS (ESI, Pos) m/z 361.10 (MH+); HPLC 0.64 min.

4.2. Biology

4.2.1. Radioligand binding assays

Competitive binding assays were performed using the non-selective benzodiazepine-site modulator [3H]flunitrazepam on recombinant Sf9 membranes co-expressing the α, β, and γ subunits of $GABA_A$ receptor in combination of α1β2γ2, α2β3γ2, α3β3γ2, or α5β3γ2, which are major benzodiazepine-sensitive α-subtypes found in CNS.[27] The test compound was incubated for 1 h at 4 °C in assay buffer (20 mM Tris–Citrate and 200 mM NaCl, pH 7.8) containing 20–100 μg of membrane protein and 3 nM of [3H] flunitrazepam in a total volume of 250 μl. The reaction was terminated by rapid filtration through PerkinElmer GF/B UniFilters. Bound radioligands were measured by liquid scintillation counting. The assay was run in parallel in presence of 10 μM of flumazenil to determine nonspecific binding.

After sigmoidal non-linear curve fitting to the data of specific binding, compound's IC_{50} values were obtained at the concentration replacing 50% of radioligand bound to the receptor. The K_i values were calculated using the equation $K_i = IC_{50}/(1 + L/K_d)$, where L is the radioligand concentration and K_d is the equilibrium dissociation constant of the radioligand.

4.2.2. Electrophysiological assays to measure functional activity of allosteric modulators of $GABA_A$ receptors

4.2.2.1. Preparation of *Xenopus* oocytes and injection of cRNA. Ovarian lobes of *Xenopus laevis* frogs were purchased from NASCO (Fort Atkinson, WI) and were torn open carefully in OR2 solution (82 NaCl, 2.5 HEPES, 1.5 NaH_2PO_4, 1 $MgCl_2$, 0.1 EDTA, in mM, pH 7.4). The oocytes were defolliculated by incubating twice in a total of 25 mL of OR2 solution containing 0.2% collagenase IA (Sigma C5894) for a total of 60 min on a test tube rocker rocking at 0.5 Hz. After several washes with OR2, oocytes were stored in 0.5× Leibovitz's L-15 medium (Sigma L1518) containing 0.1 mg/mL gentamicin (Sigma G1914), 100 units/mL of penicillin, and 0.1 mg/mL of streptomycin (Sigma P4333). Stage V or VI oocytes were selected and injected with cRNA on the same or following day. Each oocyte was injected 20–40 nL of capped and linearized cRNA containing 0.2–2 ng of α, β, or γ subunits of the human $GABA_A$ receptor genes. The cRNA ratio of α:β:γ were 1:1:10, 1:1:2, 1:1:10, and 1:1:5 by weight for $(\alpha1)_2(\beta2)_2\gamma2$,

$(\alpha2)_2(\beta3)_2\gamma2$, $(\alpha3)_2(\beta3)_2\gamma2$, and $(\alpha5)_2(\beta3)_2\gamma2$, respectively. Oocytes were used for TEVC experiments 2–10 days after injection.

4.2.2.2. Evaluate modulators by two-electrode voltage clamp recording. TEVC recording was carried out using OpusXpress 6000A (Molecular Devices, Sunnyvale, CA), which allows simultaneous recording from eight oocytes. Oocytes were perfused with ND96 (96 NaCl, 2 KCl, 1.8 $CaCl_2$, 1 $MgCl_2$, 5 HEPES, in mM, pH 7.5) at a flow rate of 2 ml/min. Oocytes were impaled with two micro-glass electrodes filled with 3 M KCl. Tip resistances of 0.5–2 MΩ and 0.5–10 MΩ were used for the current and voltage electrodes, respectively. Membrane potential was held at −60 mV. Oocytes with leak current above 50 nA at the holding potential were discarded.

To determine EC_{20} concentration of GABA for each oocyte, a series of 30 s-pulses with increasing concentrations of GABA was applied to oocytes with 4.5 min-intervals. To test a modulator, oocytes were pre-treated with the compound for 100 s before they were co-treated with GABA at EC_{20} for 30 s. A set of three pulses of GABA alone at EC_{20} prior to modulator testing was conducted and the average of the three readings was used to establish the baseline GABA response. For concentration-response curves, increasing concentrations of the modulator were applied on the same oocyte at 5 min-intervals. The GABA EC_{50} values averaged by geometric mean from eight individual oocytes for $(\alpha1)_2(\beta2)_2\gamma2$, $(\alpha2)_2(\beta3)_2\gamma2$, $(\alpha3)_2(\beta3)_2\gamma2$, and $(\alpha5)_2(\beta3)_2\gamma2$ were typically 34, 27, 63, and 17 μM, respectively.

Modulation was calculated according to the amplitude change of GABA current caused by the modulator [(current evoked by modulator + GABA/current evoked by GABA alone) −1]. The current amplitude was measured from baseline to peak using Clampfit (Molecular Devices, Sunnyvale, CA). Concentration-response curves were plotted and fitted with Prism GraphPad using sigmoidal non-linear regression with variable slopes (GraphPad Software, Inc. San Diego, CA).

4.2.3. Screening for α5-$GABA_A$R NAMs

For negative modulator screening, oocytes were treated with GABA at EC_{20} for 30 s to establish a baseline GABA response followed by a 30 s treatment with 10 μM of the test compound and GABA at EC_{20}. Eight compounds were tested on the same oocyte sequentially with 4 min intervals. For $n = 2$, one 96-well plate was assayed from A to H and another assayed from H to A to monitor interference among compounds with a throughput of 64 data points/32 compounds per run on OpusXpress 6000A. Positives were re-tested at EC_{20} of GABA to establish concentration-response curves of the test compound. Before the NAM screening, compounds were pre-screened by preset criteria for other physical properties and biological activities such as their aqueous solubility at pH7.4 and their stability in human and rat liver microsomes.

4.3. Quantum mechanical simulations

Absolute energies, equilibrium structures and harmonic vibrational frequencies were determined for each stationary point described. The B3LYP generalized gradient approximation exchange-correlation density functional was used throughout.[28,29] The 6-311G** basis set was used for all computations.[30,31] Minima and transition states were optimized via analytic gradients until the residual root mean square gradient was less than 10^{-4} hartree/bohr. The mass-weighed Hessian matrix, and hence the harmonic vibrational frequencies, were determined analytically. Minima and transition states were confirmed by the presence of zero or one imaginary frequency, respectively. All computations were carried out with the GAUSSIAN03 program package.[32]

Supplementary data

Supplementary data associated with this article can be found, in the online version, at doi:10.1016/j.bmc.2010.09.058. These data include MOL files and InChiKeys of the most important compounds described in this article.

References and notes

1. Johnston, G. A. R. *Pharmacol. Ther.* **1996**, *69*, 173.
2. Kaplan, E. M.; DuPont, R. L. *Curr. Med. Res. Opin.* **2005**, *21*, 941.
3. Depoortere, H.; Zivkovic, B.; Lloyd, K. G.; Sanger, D. J.; Perrault, G.; Langer, S. Z.; Bartholini, G. *J. Pharmacol. Exp. Ther.* **1986**, *237*, 649.
4. Leidenheimer, N. J.; Schechter, M. D. *Pharmacol. Biochem. Behav.* **1988**, *31*, 249.
5. Atack, J. R.; Wafford, K. A.; Tye, S. J.; Cook, S. M.; Sohal, B.; Pike, A.; Sur, C.; Melillo, D.; Bristow, L.; Bromidge, F.; Ragan, I.; Kerby, J.; Street, L.; Carling, R.; Castro, J. L.; Whiting, P.; Dawson, G. R.; McKernan, R. M. *J. Pharmacol. Exp. Ther.* **2006**, *316*, 410.
6. Dawson, G. R.; Maubach, K. A.; Collinson, N.; Cobain, M.; Everitt, B. J.; MacLeod, A. M.; Choudhury, H. I.; McDonald, L. M.; Pillai, G.; Rycroft, W.; Smith, A. J.; Sternfeld, F.; Tattersall, F. D.; Wafford, K. A.; Reynolds, D. S.; Seabrook, G. R.; Atack, J. R. *J. Pharmacol. Exp. Ther.* **2006**, *316*, 1335.
7. Lader, M. H. *Eur. Neuropsychopharmacol.* **1999**, *9*, S399.
8. Ashton, H. In *Adverse Syndromes and Psychiatric Drugs: A Clinical Guide*; Haddad, P., Dursun, S., Deakin, B., Eds.; Oxford University Press: Oxford, 2004; pp 239–260.
9. Rudolph, U.; Crestani, F.; Benke, D.; Brünig, I.; Benson, J. A.; Fritschy, J.; Martin, J. R.; Bluethmann, H.; Möhler, H. *Nature* **1999**, *401*, 796.
10. McKernan, R. M.; Rosahl, T. W.; Reynolds, D. S.; Sur, C.; Wafford, K. A.; Atack, J. R.; Farrar, S.; Myers, J.; Cook, G.; Ferris, P.; Garrett, L.; Bristow, L.; Marshall, G.; Macaulay, A.; Brown, N.; Howell, O.; Moore, K. W.; Carling, R. W.; Street, L. J.; Castro, J. L.; Ragan, C. I.; Dawson, G. R.; Whiting, P. J. *Nat. Neurosci.* **2000**, *3*, 587.
11. Löw, K.; Crestani, F.; Keist, R.; Benke, D.; Brünig, I.; Benson, J. A.; Fritschy, J. M.; Rülicke, T.; Bluethmann, H.; Möhler, H.; Rudolph, U. *Science* **2000**, *290*, 131.
12. Crestani, F.; Keist, R.; Fritschy, J. M.; Benke, D.; Vogt, K.; Prut, L.; Bluthmann, H.; Mohler, H.; Rudolph, U. *Proc. Natl. Acad. Sci. U.S.A.* **2002**, *99*, 8980.
13. Rudolph, U.; Möhler, H. *Curr. Opin. Pharmacol.* **2006**, *6*, 18.
14. Settimo, F. D.; Taliani, S.; Trincavelli, M. L.; Montali, M.; Martini, C. *Curr. Med. Chem.* **2007**, *14*, 2680.
15. Atack, J. R. *CNS Neurosci. Ther.* **2008**, *14*, 25.
16. Maubach, K. *Curr. Drug Targets—CNS Neurol. Disord.* **2003**, *2*, 233.
17. Collinson, N.; Atack, J. R.; Laughton, P.; Dawson, G. R.; Stephens, D. N. *Psychopharmacol.(Ber.)* **2006**, *188*, 619.
18. Atack, J. R. *Pharmacol. Ther.* **2010**, *125*, 11.
19. Chang, H. F.; Chapdelaine, M.; Dembofsky, B. T.; Herzog, K. J.; Horchler, C.; Schmiesing, R. J. WO2008155572 A2, 2008.
20. Chapdelaine, M. J.; Ohnmacht, C. J.; Becker, C.; Chang, H. F.; Dembofsky, B. T. US2007142328 A1 and WO2007073283 A1, 2007.
21. Ator, N. A.; Atack, J. R.; Hargreaves, R. J.; Burns, H. D.; Dawson, G. R. *J. Pharmacol. Exp. Ther.* **2010**, *332*, 4.
22. Porter, V. R.; Buxton, W. G.; Fairbanks, L. A.; Strickland, T.; O'Connor, S. M.; Rosenberg-Thompson, S.; Cummings, J. L. *J. Clin. Neuropsychiatry Clin. Neurosci.* **2003**, *15*, 180.
23. Jost, B. C.; Grossberg, G. T. *J. Am. Geriatr. Soc.* **1996**, *44*, 1078.
24. Lewis, D. A.; Cho, R. Y.; Carter, C. S.; Erklund, K.; Forster, S.; Kelly, M. A.; Montrose, D. *Am. J. Psychiatry* **2008**, *165*, 1585.
25. Hauser, J.; Rudolph, U.; Keist, R.; Mohler, H.; Feldon, J.; Yee, B. K. *Mol. Psychiatry* **2005**, *10*, 201.
26. Yee, B. K.; Keist, R.; von Boehmer, L.; Studer, R.; Benke, D.; Hagenbuch, N.; Dong, Y.; Malenka, R. C.; Fritschy, J. M.; Bluethmann, H.; Feldon, J.; Möhler, H.; Rudolph, U. *Proc. Natl. Acad. Sci. U.S.A.* **2005**, *102*, 17154.
27. Whiting, P. J. *Drug Discovery Today* **2003**, *8*, 445.
28. Lee, C.; Yang, W.; Parr, R. G. *Phys. Rev. B* **1988**, *37*, 785.
29. Becke, A. D. *J. Chem. Phys.* **1993**, *98*, 5648.
30. Krishnan, R.; Binkley, J. S.; Seeger, R.; Pople, J. A. *J. Chem. Phys.* **1980**, *72*, 650.
31. McLean, A. D.; Chandler, G. S. *J. Chem. Phys.* **1980**, *72*, 5639.
32. Frisch, M. J.; Trucks, G. W.; Schlegel, H. B.; Scuseria, G. E.; Robb, M. A.; Cheeseman, J. R.; Montgomery, Jr., J. A.; Vreven, T.; Kudin, K. N.; Burant, J. C.; Millam, J. M.; Iyengar, S. S.; Tomasi, J.; Barone, V.; Mennucci, B.; Cossi, M.; Scalmani, G.; Rega, N.; Petersson, G. A.; Nakatsuji, H.; Hada, M.; Ehara, M.; Toyota, K.; Fukuda, R.; Hasegawa, J.; Ishida, M.; Nakajima, T.; Honda, Y.; Kitao, O.; Nakai, H.; Klene, M.; Li, X.; Knox, J. E.; Hratchian, H. P.; Cross, J. B.; Bakken, V.; Adamo, C.; Jaramillo, J.; Gomperts, R.; Stratmann, R. E.; Yazyev, O.; Austin, A. J.; Cammi, R.; Pomelli, C.; Ochterski, J. W.; Ayala, P. Y.; Morokuma, K.; Voth, G. A.; Salvador, P.; Dannenberg, J. J.; Zakrzewski, V. G.; Dapprich, S.; Daniels, A. D.; Strain, M. C.; Farkas, O.; Malick, D. K.; Rabuck, A. D.; Raghavachari, K.; Foresman, J. B.; Ortiz, J. V.; Cui, Q.; Baboul, A. G.; Clifford, S.; Cioslowski, J.; Stefanov, B. B.; Liu, G.; Liashenko, A.; Piskorz, P.; Komaromi, I.; Martin, R. L.; Fox, D. J.; Keith, T.; Al-Laham, M. A.; Peng, C. Y.; Nanayakkara, A.; Challacombe, M.; Gill, P. M. W.; Johnson, B.; Chen, W.; Wong, M. W.; Gonzalez, C.; Pople, J. A. GAUSSIAN03, Revision C.02, Gaussian, Inc., Wallingford CT, 2004.